

Supporting information

Automated NMR assignment of protein side chain resonances using APSY

Sebastian Hiller, Rosmarie Joss and Gerhard Wider

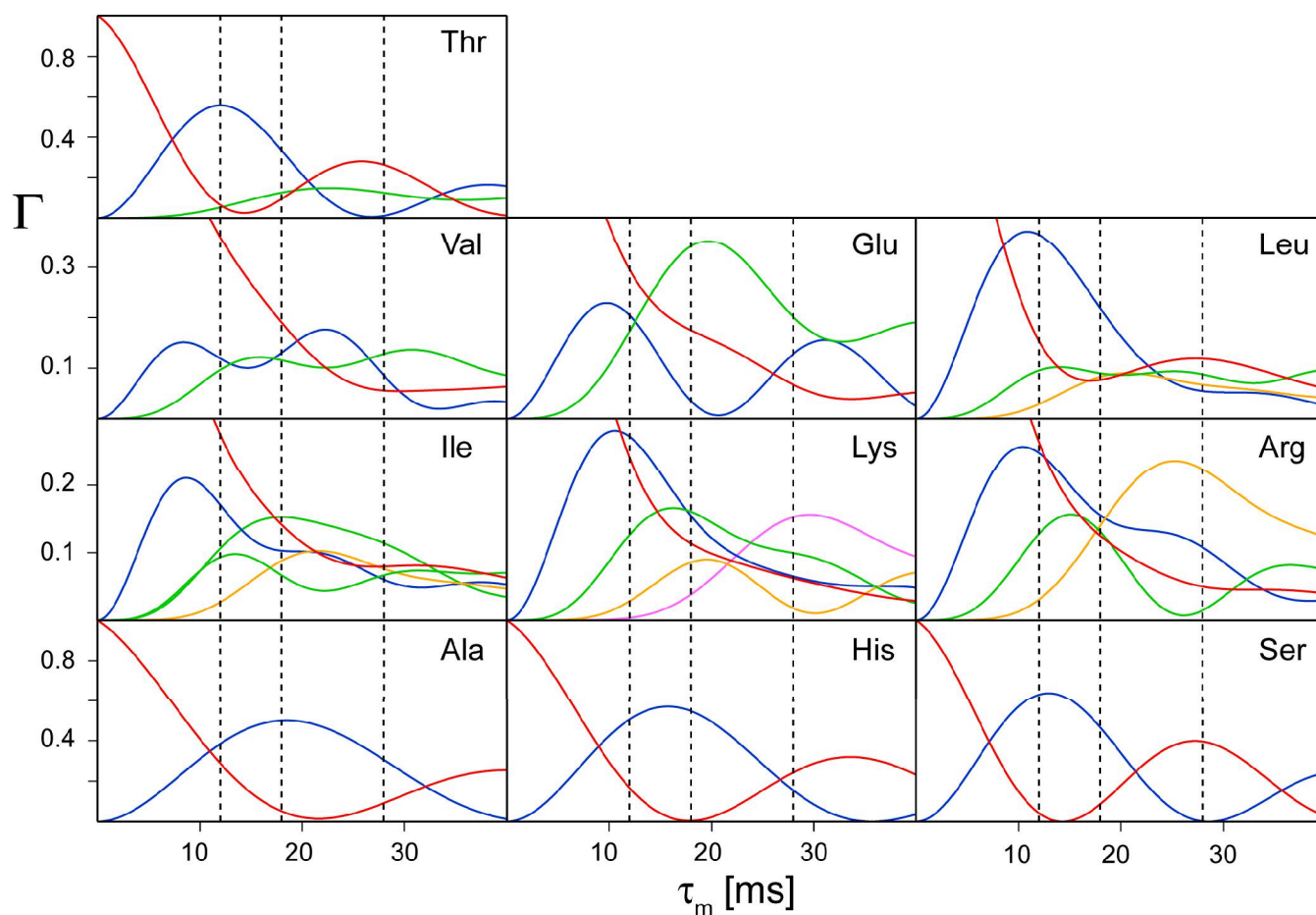


Figure S1. Calculated magnetization transfer amplitudes Γ for the carbon-carbon transfers $^{13}\text{C}^\alpha - ^{13}\text{C}^\alpha$ (red), $^{13}\text{C}^\beta - ^{13}\text{C}^\alpha$ (blue), $^{13}\text{C}^\gamma - ^{13}\text{C}^\alpha$ (green), $^{13}\text{C}^\delta - ^{13}\text{C}^\alpha$ (yellow) and $^{13}\text{C}^\epsilon - ^{13}\text{C}^\alpha$ (magenta) during isotropic mixing in the HC(CC-TOCSY)CONH experiment. The calculations were done as described in Materials and Methods. The vertical dashed lines indicate the three mixing times used in the present work (12ms, 18ms and 28ms). The transfer functions for Ala, His and Ser are representative for the ten

two-carbon spin systems of the amino acids Ala, Asn, Asp, Cys, His, Phe, Ser, Trp and Tyr. The three examples Ala, Ser and His are the systems with the smallest, the largest and an intermediate effective C-C coupling, respectively. The data for Gln and Met are very similar to Glu. The data for Pro (Fig. S2) corresponds to Arg.

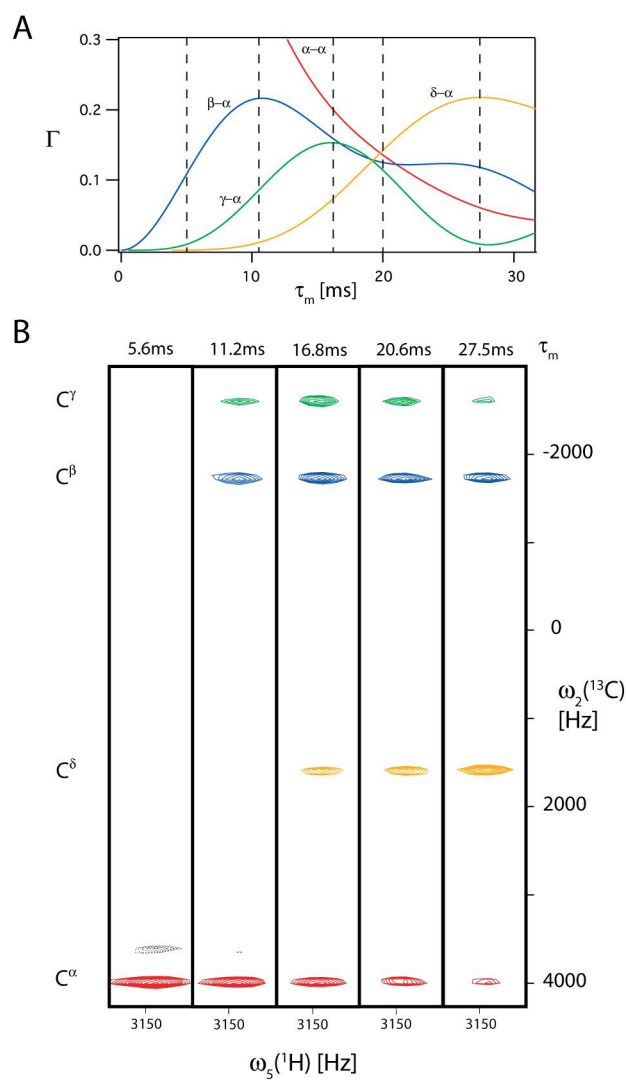


Figure S2. (A) Calculated magnetization transfer amplitudes Γ for the carbon-carbon transfers in proline residues during isotropic mixing in the HC(CC-TOCSY)CONH experiment. (B) Strips from five 2D $(\omega_2(^{13}\text{C}), \omega_5(^1\text{H}))$ -projections of the 5D APSY-HC(CC-TOCSY)CONH experiment for Pro 41 of 434-repressor(1–63). The five experiments were recorded with different mixing times, as indicated above each strip. The cross peaks of C^α , C^β , C^γ and C^δ are colored red, blue, green and yellow, respectively.

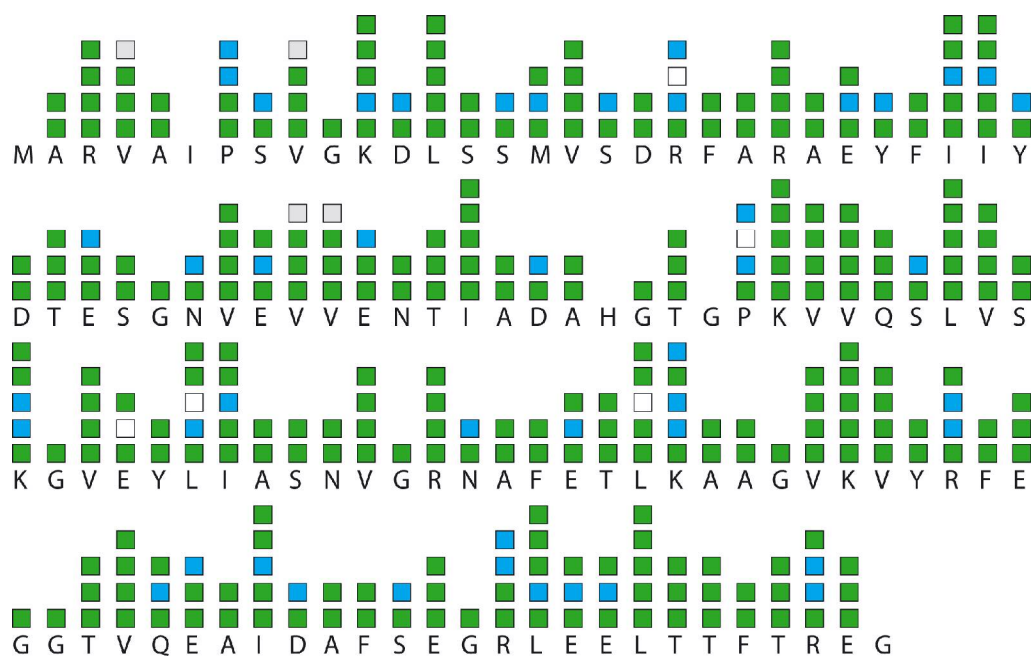


Figure S3. Graphical illustration of the aliphatic side chain assignments obtained for TM1290 based on a 5D APSY-HC(CC-TOCSY)CONH using 2D projection spectra and the backbone $^1\text{H}^{\text{N}}$, ^{15}N and ^{13}C assignments. Squares represent the aliphatic side chain carbons and the C^{α} of each amino acid. Residues without squares can either not be detected by the experiment or are also not represented in the reference assignment established with conventional spectra. Green squares represent carbon atoms, where all expected proton shifts are found, i.e. two proton shifts for CH_2 and one for CH and CH_3 groups. Blue squares indicate CH_2 groups, for which only one proton shift was found. No peak was found for the white squares. Grey squares indicate isopropyl methyl groups that were not detected.

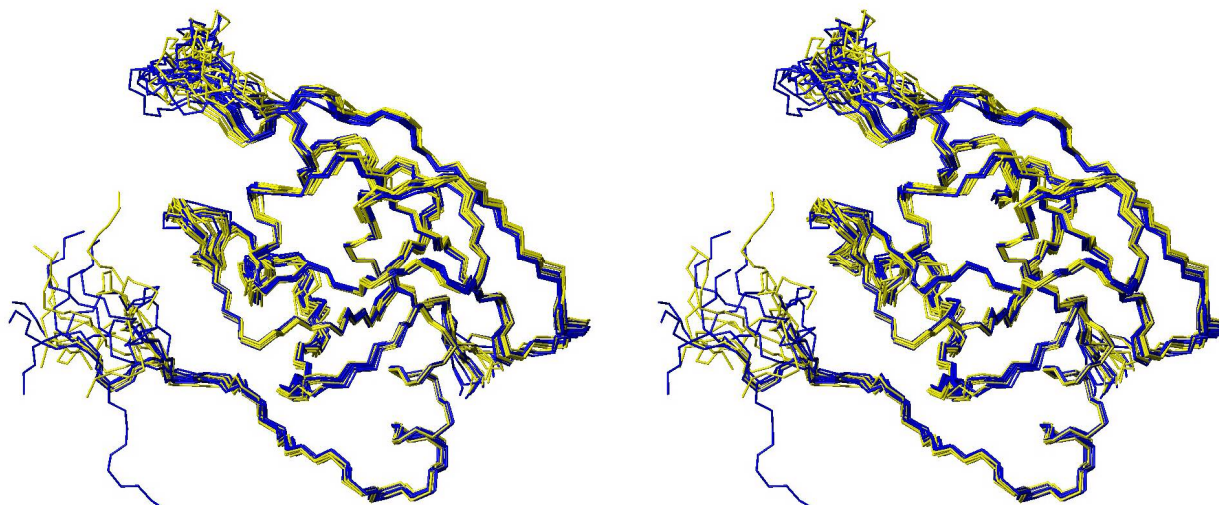


Figure S4. Stereo view of two superimposed backbone bundles of the protein TM1290. Each bundle shows the 10 lowest-energy conformers from 100 calculated CYANA structures. Blue: Calculation with the 2444 upper limit constraints corresponding to the complete manual assignment.¹ Yellow: Calculation with the same input data except the NOEs of all aliphatic atoms that were not assigned in the present work (2159 upper limit constraints). The RMSDs for heavy atoms of residues 3–43 and 52–110 are 0.82 ± 0.07 Å and 0.84 ± 0.07 Å, for the blue and yellow bundle, respectively, and 0.88 ± 0.07 Å for the combined bundle of 20 conformers.

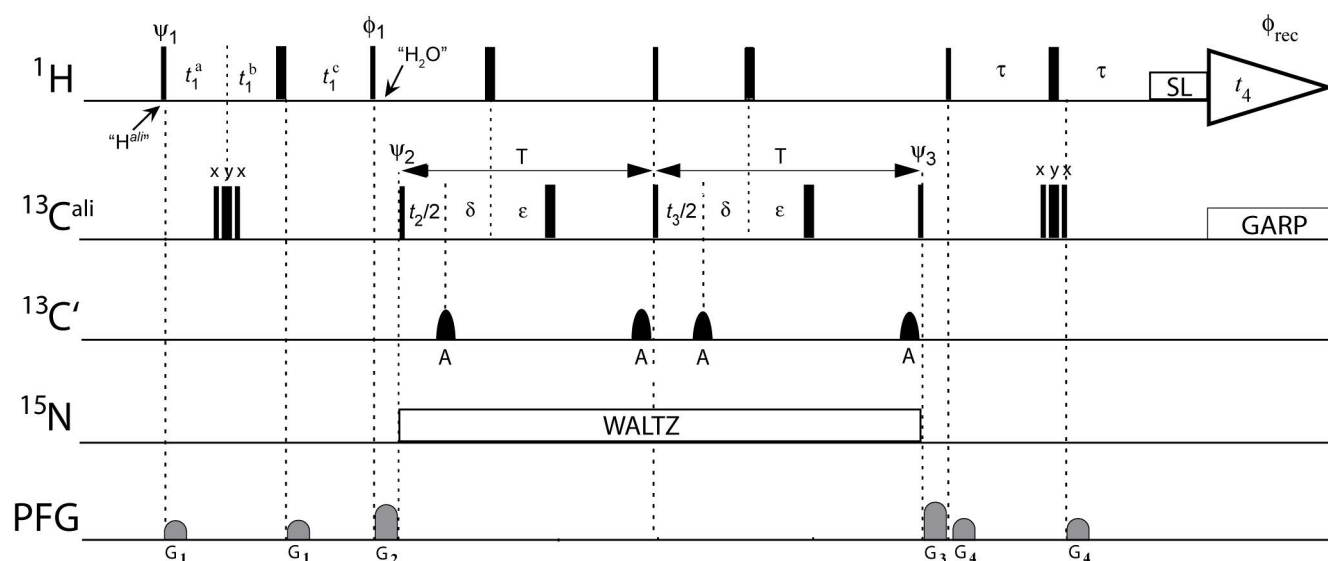


Figure S5. Pulse sequence of the 4D APSY-HCCH-COSY experiment. Radio-frequency (rf) pulses were applied at 39 ppm for aliphatic carbon nuclei, $^{13}\text{C}^{\text{ali}}$, at 174 ppm for carbonyl carbons, $^{13}\text{C}'$, and 119 ppm for ^{15}N . The carrier frequency for protons was set in the aliphatic region at 2.5 ppm at the beginning of the experiment, indicated on the line ^1H by " H^{ali} "; at the position " H_2O " the carrier was set to the water resonance (4.7 ppm). Bars stand for rectangular pulses applied at maximum power; the thin bars represent 90° pulses and the wide bars 180° pulses. Shaped rf pulses on the line $^{13}\text{C}'$ marked with A are 180° Gauss pulses (5% truncation) with a duration of $120\mu\text{s}$ on a 750 MHz spectrometer. The decoupling sequences WALTZ-16² on ^{15}N and GARP³ on C^{ali} are indicated with white rectangles. The triangle labeled t_4 represents the acquisition period. The spin lock pulse before the acquisition is shown as a rectangle marked "SL". On the line marked PFG, curved shapes indicate sine bell shaped, pulsed magnetic field gradients along the z-axis with the following durations and strengths: G_1 : $400\mu\text{s}$, 40%; G_2 : $800\mu\text{s}$, 50%; G_3 : $1000\mu\text{s}$, 70%; G_4 : $600\mu\text{s}$, 45%. The initial delays in the evolution periods were $t_1^{\text{a}} = t_1^{\text{c}} = 1.6\text{ms}$, $t_1^{\text{b}} = 5\mu\text{s}$ and $t_2/2 = t_3/2 = 10\mu\text{s}$. Further delays were $\delta = 1.1\text{ms}$, $\varepsilon = 2.8\text{ms}$ and $\tau = 1.6\text{ms}$. The constant time period T was set to 7.8ms. All pulse were applied with phase x unless indicated otherwise above the pulse. The following phase cycles were used: $\phi_1 = \{y, y, -y, -y\}$, $\psi_3 = \{x, -x\}$ and $\phi_{\text{rec}} = \{x, -x, -x, x\}$. Quadrature detection for the indirect dimension was achieved with the phases ψ_1 , ψ_2

and ψ_3 for t_1 , t_2 and t_3 , respectively. These phases were simultaneously incremented in 90° steps for consecutive FID's. Quadrature detection for the indirect dimensions was achieved using the trigonometric addition theorem to obtain pure cosine and sine terms for a subsequent hypercomplex Fourier transformation.^{4, 5} The pulse phases ψ_1 , ψ_2 and ψ_3 were incremented in 90° -steps for t_1 , t_2 and t_3 , respectively; only the pulse phases of the evolution periods which are part of the given projection are incremented.

Table T1. List of the 42 BMRB entries used for statistical chemical shift data analysis in this work.

| Entry No. | Protein name | Year | Residues |
|-----------|--|------|----------|
| bmr4050 | Rubredoxin | 1997 | 54 |
| bmr4068 | Turkey ovomucoid third domain | 1998 | 56 |
| bmr4070 | FimC | 1998 | 205 |
| bmr4081 | Interferon-alpha-2a | 1997 | 165 |
| bmr4092 | Core binding factor b subunit | 1998 | 143 |
| bmr4117 | Human Elongation Factor-1beta | 1998 | 91 |
| bmr4126 | Single chain three helix bundle | 1999 | 73 |
| bmr4140 | EH1 domain of mouse Eps15 | 1998 | 120 |
| bmr4146 | F1Fo ATP Synthase Subunit c | 1998 | 79 |
| bmr4154 | Oxidized putidaredoxin | 1999 | 106 |
| bmr4156 | Protein Disulfide Isomerase | 1999 | 110 |
| bmr4184 | Eps15 homology domain | 1998 | 95 |
| bmr4205 | Ets-1 Pointed | 1998 | 110 |
| bmr4223 | TATA box binding protein associated factor II 230 | 1998 | 67 |
| bmr4237 | MinE topological specificity domain | 1999 | 58 |
| bmr4249 | Human NER factor XPA | 1998 | 122 |
| bmr4284 | Calmodulin-Ca ²⁺ Pump-Peptide Complex | 1999 | 148 |
| bmr4296 | Major cold shock protein from E. coli | 1998 | 70 |
| bmr4302 | Protein disulfide isomerase a' domain | - | 115 |
| bmr4311 | Human T-cell leukemia virus type I capsid monomer | 1999 | 214 |
| bmr4313 | ARD | 2002 | 179 |
| bmr4317 | NS1(1-73) dimmer | 1997 | 73 |
| bmr4318 | Glutaredoxin 2 | 1999 | 215 |
| bmr4326 | N-Terminal Domain of DNA Polymerase B | 1994 | 87 |
| bmr4327 | N-Terminal inhibitory domain of metalloproteinases-1 inhibitor | 1999 | 126 |
| bmr4334 | ARID domain of dead-ringer protein | 1999 | 139 |
| bmr4371 | Recombinant Onconase/P30 protein | 1999 | 105 |

| | | | |
|---------|--|------|-----|
| bmr4395 | Ribosomal protein L25 | 1998 | 94 |
| bmr4401 | Skeletal N-troponin C | 1998 | 90 |
| bmr4437 | Merozoite surface protein 1 | 1999 | 96 |
| bmr4455 | CD58 adhesion domain, 1dCD58 | 1999 | 95 |
| bmr6655 | Zinc finger domains 1 and 2 of dsRBP-ZFa | 2005 | 127 |
| bmr6751 | Asl1650 | 2006 | 88 |
| bmr6868 | Protein ydhR precursor | 2005 | 123 |
| bmr6955 | Hypothetical protein ydhA | 2006 | 102 |
| bmr7014 | Nsp1 | 2006 | 116 |
| bmr7080 | NTD-CTD complex | 2006 | 33 |
| bmr7106 | RGS18 monomer | 2003 | 151 |
| bmr7119 | 32324 monomer | 2006 | 189 |
| bmr7170 | Sr482 monomer | - | 117 |
| bmr7191 | Pat90 monomer | - | 97 |
| bmr7229 | Small inducible cytokine B14 | 2006 | 78 |

References

- (1) Etezady-Esfarjani, T.; Herrmann, T.; Peti, W.; Klock, H. E.; Lesley, S. A.; Wüthrich, K. *J. Biomol. NMR* **2004**, *29*, 403–406.
- (2) Shaka, A. J.; Keeler, J.; Frenkiel, T.; Freeman, R. *J. Magn. Reson.* **1983**, *52*, 335–338.
- (3) Shaka, A. J.; Barker, P. B.; Freeman, R. *J. Magn. Reson.* **1985**, *64*, 547-552.
- (4) Brutscher, B.; Morelle, N.; Cordier, F.; Marion, D. *J. Magn. Reson. B* **1995**, *109*, 238–242.
- (5) Kupce, E.; Freeman, R. *J. Am. Chem. Soc.* **2004**, *126*, 6429–6440.